Time of Arrival Based Localization of UWB Transmitters Buried in Lossy Dielectric Media

Michael Mirbach, Wolfgang Menzel
Institute of Microwave Techniques, University of Ulm, PO Box, 89069 Ulm, Germany
michael.mirbach@uni-ulm.de

***Abstract*—An algorithm for subsurface localization of UWB transmitters in homogeneous dielectric media is presented. In combination with surface estimation algorithms for UWB pulse radars it allows localization behind arbitrarily shaped medium surfaces. We propose a localization system operating in the FCC UWB frequency range from 3.1 to 10.6 GHz consisting of a transmitter optimized for radiation in high permittivity media and of external radar sensors. The sensors scan the dielectric surface and also measure the time of arrival (ToA) of the signal transmitted from inside of the medium. The transmitter location is estimated by combining the measured ToA data with the knowledge about shape and position of the medium. Therefore a method to calculate wavefront refraction on the medium boundary based on the Huygens-Fresnel principle is derived. The performance of the proposed localization method is verified using electro-magnetic field simulations and measurements. The measurements have been performed with the transmitter placed in high permittivity tissue-mimicking liquid. The localization results are compared with the manually measured transmitter position showing a good agreement.**

***Index Terms*—Localization, surface estimation, ultra-wideband (UWB) pulse radar, wave propagation**

I. Introduction

Ultra-wideband (UWB) pulse-based radio has a great potential in medical sensing and imaging applications due to its high range resolution and good non-destructive penetration abilities of dielectric materials. In this context, a main focus of research is put on imaging of high permittivity scattering centers in human tissue, e.g. in breast cancer detection [1]. In this paper we investigate an inverse approach: The localization of actively transmitting beacons inside of the human body, starting with investigations based on tissue-mimicking media. An application could be the tracking of catheters equipped with UWB transmitters. The use of active transmitters would mitigate the challenges related to the high attenuation of electro-magnetic waves in human tissue, which makes purely passive localization extremely difficult [2].

A similar approach has been investigated in the field of ultrasonics, where catheter-mounted ultrasound transducers in combination with external arrays of imaging transducers are used to track the catheter position [3], [4]. The advantage of UWB catheter localization is a contactless measurement setup with receivers placed in air around the patient while ultrasound transducers have to be placed directly on the body.

In most through-dielectric localization problems, like through-the-wall imaging, a plane boundary between air and the target medium is assumed [5], [6]. A human body, however, cannot be considered as a plane surface. Therefore, the exact body shape has to determined prior to localization. We thus propose a system consisting of a sensor array which acts as both a surface scanner and a receiver recording the time of arrival (ToA) of a signal transmitted from the catheter.

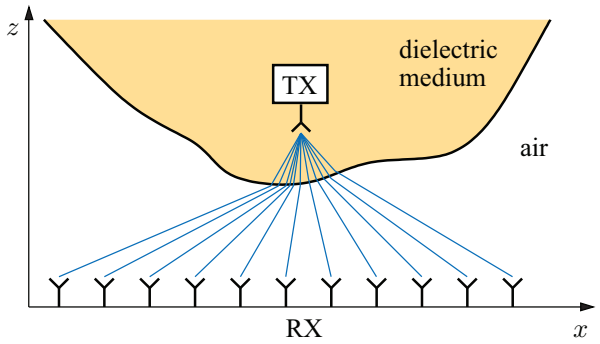

Fig. 1. 2D localization problem of a RF transmitter buried in a high permittivity dielectric medium. The path of wave propagation between the transmitter and the receivers distributed along the x-axis is described by rays.

Several methods to estimate the surface of a highly reflective medium using UWB pulse radar sensors have been investigated in recent years [7], [8]. In this paper, building on these surface estimation methods, we present a new approach for the localization of transmitters inside of an arbitrarily shaped homogeneous dielectric medium taking into account its previously determined surface profile.

II. Proposed Localization Setup

In subsurface imaging and localization problems, where sensors are not directly in contact with the medium, the permittivity contrast between air and the medium cannot be neglected as it leads to a different wave propagation velocity inside of the material and hence to refraction effects at its surface. This is illustrated in Fig. 1. In case of medical applications a relative permittivity of human tissue between 30 and 50 in the FCC UWB frequency range has to be considered [9]. UWB signals are therefore strongly reflected at the air-to-body interface. These reflections are beneficial to surface estimation applications using UWB pulse radars. For in-body localization, however, they constrain a signal emission from inside of the body. This is why we propose a system that combines an array of radar transceivers outside of the body with active transmitters inside of the body to overcome strong

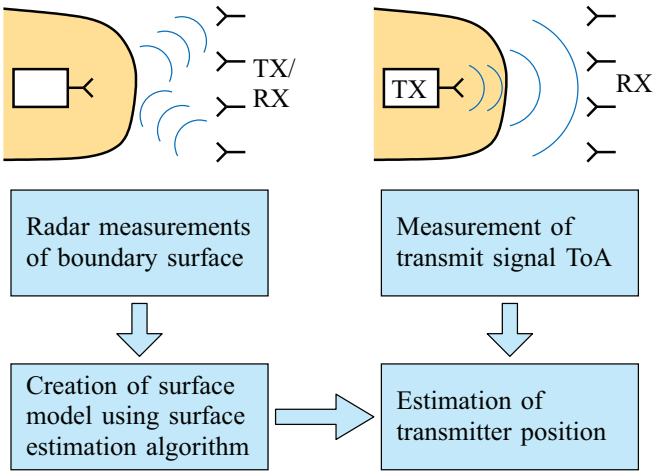

Fig. 2. Proposed localization procedure of a transmitter buried in a dielectric medium. In the first step the sensor array is used to scan the surface (left), in the second step it only receives the transmitted signal (right).

reflection losses.

Fig. 2 summarizes the proposed localization approach of a transmitter placed in a dielectric medium. In a first step, the array of radar sensors is used to measure the distance to the boundary surface. These measured distances together with the known antenna positions are the input of a surface estimation algorithm which returns a model of the boundary surface. In the second step, the transmitter inside of the dielectric is switched on and the radar sensors operate in receive mode recording the ToA of the transmitted signal. Finally, the acquired data is combined and the position of the transmitter is determined using the localization algorithm described below.

III. Localization Algorithm

The given parameters of the localization problem are the shape of the dielectric medium containing the transmitter, its distance to the antenna array and the ToA of the localization signal at each array element. Since the wave propagation effects are reciprocal, our problem can also be regarded in a reverse way: At each receiver position the transmission of a short pulse with a delay corresponding to the respective previously measured ToA is assumed. In order to get the original beacon position we have to find the spot where all these virtual pulses would superimpose, i.e. the intersection of the impulse wavefronts inside of the medium.

One way to solve this imaging problem is a combination of Snell's Law and ray tracing where the direction and length of refracted propagation paths is evaluated [10]. This, however, involves high computational effort since the normal vector at every considered surface point has to be calculated first. Therefore a different way to determine the wavefronts of impulses transmitted into a dielectric medium is investigated here.

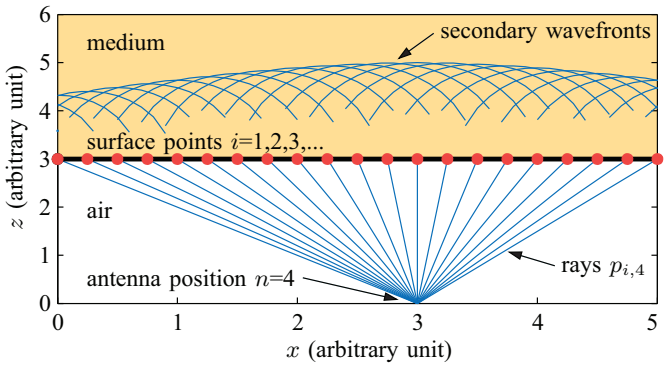

Fig. 3. Method to determine the 2D wavefront shape inside of a medium with $\varepsilon_r = 30$ of a signal transmitted in air at position $(3, 0)$. The envelope of radial waves originating from medium surface points forms the new wavefront.

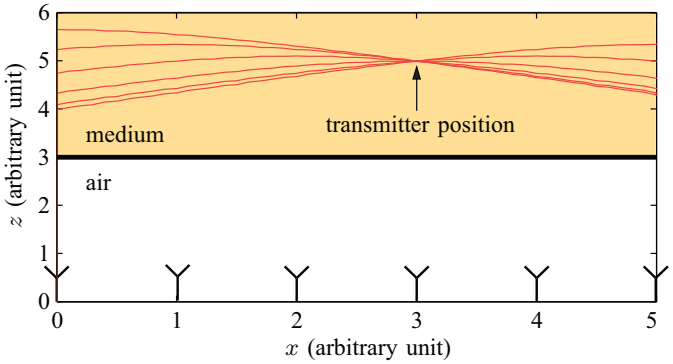

Fig. 4. Wavefronts corresponding to six different antenna positions. The intersection of the wavefronts leads to the transmitter location at $(3, 5)$.

A. Procedure of 2D Localization

According to the Huygens-Fresnel principle a refracted wavefront can be represented by an infinite number of spherical waves which originate from points on the boundary surface reached by the incoming wave. This is shown in Fig. 3 for a pulse transmitted from an antenna at position $(3, 0)$ towards a dielectric half space. In this 2D example 20 source points of radial waves on the dielectric surface are considered. The radii $r_{i,n}$ of the secondary waves are calculated from the measured ToA at the receiving antenna n and the length of the ray $p_{i,n}$ between the antenna and the surface point i:

$$r_{i,n} = \frac{1}{\sqrt{\varepsilon_r}} \left(c_0 \cdot \mathrm{ToA}_n - p_{i,n} \right), \tag{1}$$

where c_0 is the speed of light. The division by $\sqrt{\varepsilon_r}$ accounts for the different wave propagation speed in the dielectric medium. The envelope of all radial waves corresponds to the wavefront we are looking for. By repeating the procedure for every antenna element of the receiver array we get a set of wavefronts as illustrated in Fig. 4. Finally we determine the intersection of these wavefronts to obtain the transmitter position inside of the medium. A 3D localization problem is solved in an analog way with envelopes of spheres leading to intersecting 3D wavefronts. Here, however, the derivation of

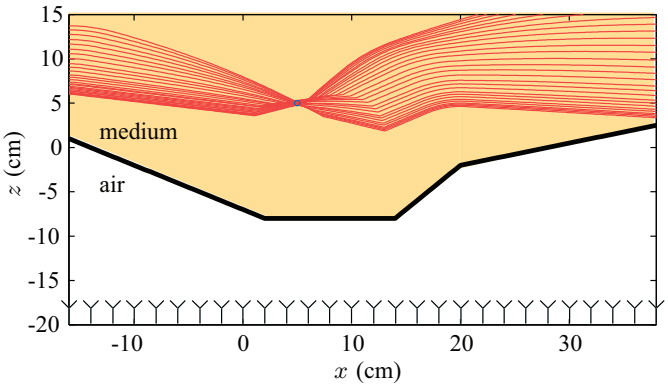

Fig. 5. Calculated wavefronts in a medium with $\varepsilon_r = 10$ based on EM field simulations. The receiving antennas are placed along the x-axis at $z = -20$, the transmitter is positioned at (5 cm, 5 cm).

the localization algorithm is limited to the 2D case because of a simpler graphical representation.

B. Verification with a Complex Surface

The wavefront shapes in Fig. 4 agree with a hyperbolic approximation of wavefronts in dielectric half spaces [11]. With more complex boundaries, however, the analytical calculation of refracted wavefronts is no longer practical, while the approach presented here is independent of the surface shape. An example of a transmitter placed behind a more complex surface is presented in Fig. 5. The times of flight between the transmitter at (5 cm, 5 cm) and the individual elements of the receiver array at $z = -20$ are calculated using electro-magnetic field simulation software [12].

The proposed 2D localization procedure leads to a belt of refracted wavefronts with a focussing point where the receiver has been placed in the simulation. To decrease calculation time it is also possible to search for the narrowest point in the wavefront belt instead of calculating the intersections. The estimated transmitter position by applying this method is (4.60 cm, 4.94 cm), having an error of about 4 mm.

It is obvious that in the example of Fig. 5 a smaller number of wavefronts and thus less receiving antennas would be sufficient to localize the transmitter. But in practical applications this high number of antennas might still be required as a dense sensor array is rather needed for surface estimation than for solving the localization problem.

IV. Measurement Results

A. Measurement Setup

The measurements are performed using custom built antennas and radar sensors operating in the FCC UWB frequency range from 3.1 to 10.6 GHz. The measurement setup is illustrated in Fig. 6. A miniaturized antenna optimized for radiation in human tissue [13] is placed as a transmitter in a container filled with a 50% sugar solution. The dielectric properties of this liquid are similar to those of human skin tissue having a relative permittivity of $\varepsilon_r \approx 30$ and an attenuation of about 23 $\frac{\text{dB}}{\text{cm}}$ at the center of the considered frequency band. The

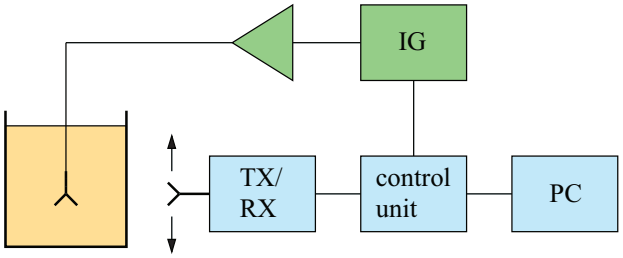

Fig. 6. Measurement setup consisting of an omni-directional antenna placed in a container with tissue-mimicking liquid and an external transceiver of variable position. The control unit provides the clock signals for the impulse generators and A/D conversion of measurement signals.

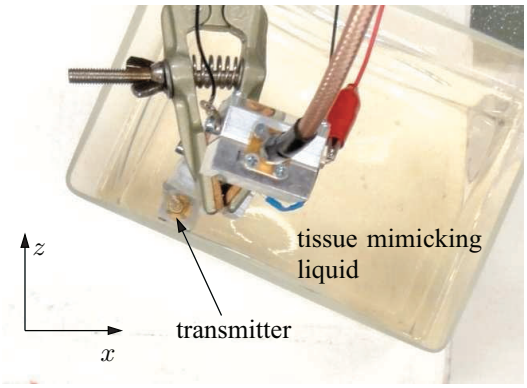

Fig. 7. Top view of the 2D measurement setup. The transmitter is positioned behind the surface of a glass container filled with tissue-mimicking liquid.

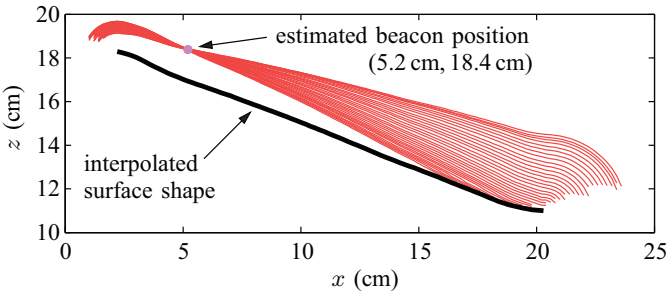

Fig. 8. Estimated refracted wavefronts corresponding to 31 receivers at $z = 0$. The beacon is localized by evaluating the intersections of the wavefronts.

transmitted signal generated by the impulse generator (IG) is a 5th order derivative of a Gaussian pulse. Because of the high attenuation of the medium an additional amplifier with 16 dB gain is applied. Outside of the container a radar sensor equipped with a correlation receiver is used to scan the container surface and measure the ToA of a transmitted impulse [14]. In this setup we emulate a whole sensor array with a single radar sensor moving in front of the container. A control unit providing clock signals for the impulse generator and the receiver is connected to a computer where the signal processing and visualization is performed. During the first step of the localization procedure – the radar scan of the container surface – the impulse generator and the amplifier in the upper part of Fig. 6 are switched off.

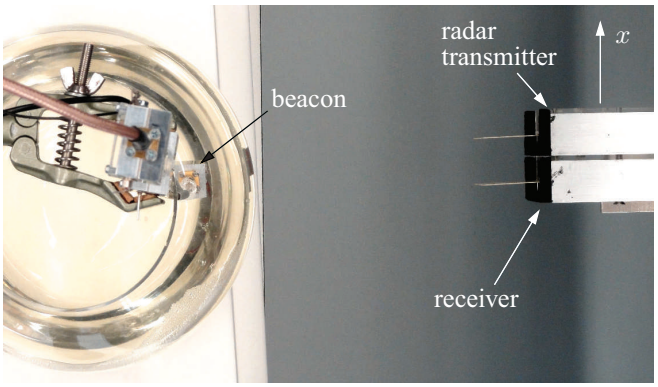

(a) Top view

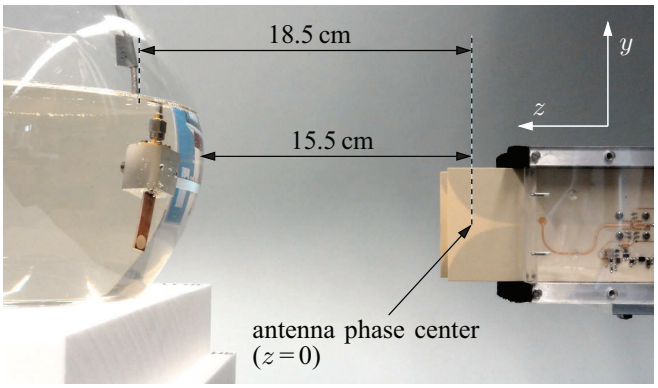

(b) Side view

Fig. 9. Photographs of the 3D measurement setup with a transmitter placed in a concave liquid container. The distances between the receiver antenna, the container and the transmitter antenna are measured manually. The receiver is positioned at the coordinates $x = 3$ cm, $y = -19$ cm.

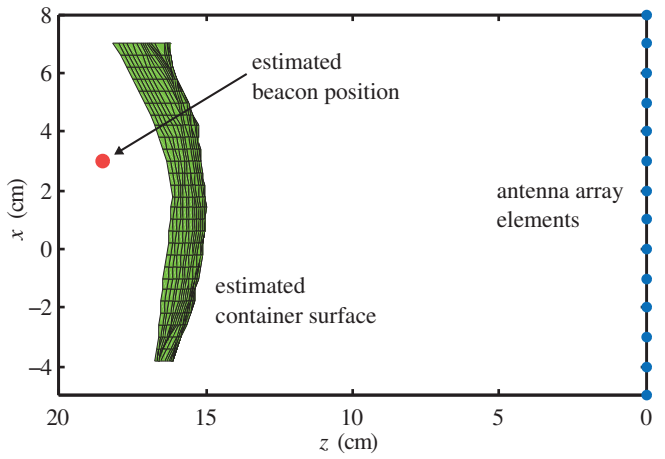

(a) Top view

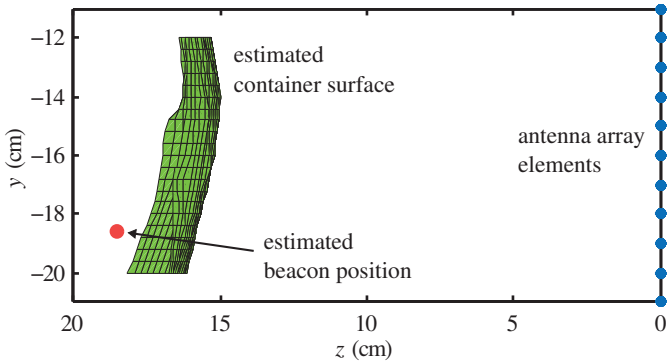

(b) Side view

Fig. 10. Measurement results in a top and side view corresponding to the photographs in Fig. 9 showing the estimated location of the beacon behind the container surface. The dots at $z = 0$ represent the sensor positions.

B. Measurements in 2D

In the first practical evaluation of the localization functionality we use a simple setup of a transmitter placed close to the surface of a slightly aslant rectangular glass container. The container is filled with tissue-mimicking liquid as shown in Fig. 7. In this 2D measurement the radar sensor is scanning the target area along the x-axis emulating a linear sensor array. For the estimation of the container shape we apply a fast imaging algorithm for bistatic pulse radar sensors based on trilateration [8]. The output of the algorithm is a scattered point cloud which is interpolated to generate a smooth surface.

This interpolated 2D surface shape is illustrated in Fig. 8. It serves for the calculation of the refracted wavefronts. We can see that most of the wavefronts intersect in one point where thus the transmitter position is assumed. The estimated position at a distance of about 1.3 cm from the container surface qualitatively agrees with the photography of the measurement setup in Fig. 7.

C. Measurements in 3D

For 3D measurements a concave liquid container which better approximates the surface of a human body is chosen. Fig. 9 shows a top and side view of the measuring setup with the transmitter placed in a glass fish bowl of 21 cm diameter. The radar sensor is scanning in 1 cm steps in x- and y-direction simulating an antenna array with in total 14×11 elements.

The surface points calculated by the trilateration-based imaging algorithm are interpolated to create the boundary shape depicted in Fig. 10. These graphs follow the perspectives of the photographs in Fig. 9 allowing a rough evaluation of the localization result. The estimated position of the transmitter based on the examination of 3D wavefronts inside of the medium is $(x, y, z) = (3.0\,\text{cm}, -18.4\,\text{cm}, 18.5\,\text{cm})$. Even though an exact verification of the antenna position inside of the liquid is difficult, the manually measured z-distance of 18.5 cm between the transmitter and the receiver agrees with the estimated beacon position. In the photographs of Fig. 9 the receiver antenna is positioned at the x- and y-position closest to the beacon antenna in the container. These known sensor coordinates of (3 cm, -19 cm) coincide well with the estimated beacon position. In case of a convex surface like the fish bowl an even better localization can be expected when using a circular arrangement of the receivers around the medium, instead of a planar one.

Due to the high attenuation of signals transmitted through

tissue-mimicking liquid we can only localize positions close to the container surface. In our measurements the signal-to-noise ratio of impulses running through more than 3 cm of tissue-mimicking liquid became too low to be detected. One possible way to increase the maximum transmitter distance from the surface would be the use of a cascade of multiple amplifiers to realize a higher transmitter power output. Regarding the optimization of signal processing an approach based on compressed sensing is investigated to cope with lower signal-to-noise ratios at the receiver [15].

V. Conclusion

In this paper a method for the localization of UWB transmitters buried in homogeneous dielectric media has been presented. With the aid of surface estimation algorithms a localization behind an arbitrarily shaped medium boundary is possible. For this purpose we have proposed a system consisting of an array of UWB radar sensors outside of the medium and a beacon inside of the medium transmitting a short UWB pulse. The external sensors serve for surface scanning and for measuring the time of arrival (ToA) of the transmitted signal. The beacon is localized by evaluating the measured ToA while considering the refraction of wavefronts on the dielectric surface. The performance of the proposed localization algorithm has been verified using electro-magnetic field simulations and measurements with the transmitter placed in high permittivity tissue-mimicking liquid. Comparisons of the localization results with the manually measured beacon position have shown a good agreement.

Acknowledgment

This work has been funded by the German Research Foundation (DFG) under the program UKoLoS.

References

[1] X. Li, E. J. Bond, B. D. V. Veen, and S. C. Hagness, "An overview of ultra-wideband microwave imaging via space-time beamforming for early-stage breast-cancer detection," *IEEE Antennas and Propagation Magazine*, vol. 47, no. 1, pp. 19–34, 2005.

[2] C. G. Bilich, "UWB radars for Bio-Medical Sensing: Attenuation Model for Wave Propagation in the body at 4GHz," *University of Trento, Italy. Technical report # DIT-06-051*, 2006.

[3] C. L. Merdes and P. D. Wolf, "Locating a catheter transducer in a three-dimensional ultrasound imaging field," *Biomedical Engineering, IEEE Transactions on*, vol. 48, no. 12, pp. 1444–1452, 2001.

[4] J. Mung, S. Han, F. Weaver, and J. Yen, "Time of flight and FMCW catheter localization," in *Ultrasonics Symposium (IUS), 2009 IEEE International*, 2009, pp. 590–593.

[5] F. Ahmad and M. G. Amin, "Noncoherent approach to through-the-wall radar localization," *IEEE Transactions on Aerospace and Electronic Systems*, vol. 42, no. 4, pp. 1405–1419, 2006.

[6] R. Salman and I. Willms, "In-Wall Object Recognition based on SAR-like Imaging by UWB-Radar," in *EUSAR 2010*, 2010.

[7] S. Kidera, T. Sakamoto, and T. Sato, "Accurate UWB Radar Three-Dimensional Imaging Algorithm for a Complex Boundary Without Range Point Connections," *Geoscience and Remote Sensing, IEEE Transactions on*, vol. 48, no. 4, pp. 1993–2004, 2010.

[8] M. Mirbach and W. Menzel, "A simple surface estimation algorithm for UWB pulse radars based on trilateration," in *ICUWB 2011, 2011 IEEE International Conference on Ultra-Wideband*, 2011, pp. 273–277.

[9] S. Gabriel, R. W. Lau, and C. Gabriel, "The dielectric properties of biological tissues: II. Measurements in the frequency range 10 Hz to 20 GHz," *Phys. Med. Biol.*, vol. 41, p. 2251, 1996.

[10] K. Akune, S. Kidera, and T. Kirimoto, "Fast and accurate imaging algorithm for targets buried in dielectric medium for UWB radars," in *General Assembly and Scientific Symposium, 2011 XXXth URSI*, 2011, pp. 1–4.

[11] C. Rappaport, "A simple approximation of transmitted wavefront shape from point sources above lossy half spaces," in *IGARSS '04, 2004 IEEE International Geoscience and Remote Sensing Symposium*, vol. 1, 2004, pp. 421–424.

[12] *CST MICROWAVE STUDIO®, User Manual*, CST Computer Simulation Technology AG, Darmstadt, Germany, 2011.

[13] M. Leib, M. Frei, D. Sailer, and W. Menzel, "Design and characterization of a UWB slot antenna optimized for radiation in human tissue," in *ICUWB 2009, IEEE International Conference on Ultra-Wideband, 2009*, 2009, pp. 159–163.

[14] M. Leib, E. Schmitt, A. Gronau, J. Dederer, B. Schleicher, H. Schumacher, and W. Menzel, "A compact ultra-wideband radar for medical applications," *Frequenz*, vol. 63, no. 1-2, pp. 2–8, 2009.

[15] T. Thiasiriphet, M. Ibrahim, and J. Lindner, "Compressed sensing for uwb medical radar applications," in *ICUWB 2012, 2012 IEEE International Conference on Ultra-Wideband*, 2012.